

Strain relief in linearly graded composition buffer layers: A design scheme to grow dislocation-free ($<10^5 \text{ cm}^{-2}$) and unstrained epilayers

S. I. Molina, F. J. Pacheco, D. Araújo, and R. García

Departamento de Ciencia de los Materiales e I. M. y Q. I., Universidad de Cádiz, Apdo. 40 11510-Puerto Real (Cádiz), Spain

A. Sacedón and E. Calleja

Departamento de Ingeniería Electrónica, Universidad Politécnica de Madrid, Ciudad Universitaria, 28040-Madrid, Spain

Z. Yang and P. Kidd

Department of Materials Science and Engineering, University of Surrey, Guilford GU2 5XH, United Kingdom

(Received 2 June 1994; accepted for publication 6 September 1994)

The strain relaxation in linearly graded composition InGaAs layers grown on (001) GaAs substrates by molecular beam epitaxy is studied by transmission electron microscopy (TEM) and double crystal x-ray diffraction (DCXRD). The dislocation distribution in these layers does not coincide with the predicted equilibrium dislocation distribution [J. Tersoff, *Appl. Phys. Lett.* **62**, 693 (1993)]. The dislocation density in the dislocation-rich layer thickness is slightly smaller than the equilibrium density. The thickness of the dislocation-rich region is different in the $[110]$ and $[1\bar{1}0]$ directions. A good correspondence exists between the TEM and DCXRD strain measurements. The dislocation distribution observed by TEM has made it possible to design a scheme to grow dislocation-free and unstrained top layers on linearly graded composition buffer layers. © 1994 American Institute of Physics.

The presence of dislocations in semiconductor active layers usually degrades the device properties. In lattice mismatched semiconductor heteroepitaxies, dislocations are generated when the epilayer surpasses a rather small critical thickness. This fact justifies the high number of research works aimed to avoid dislocation threading up to the epilayer surface of heteroepitaxial systems. To filter threading dislocations, the most widely used solutions were the growth of a single or multiple uniform composition layers between substrates and top layers,^{1,2} or the use of graded composition layers.^{3,4}

Recently, Tersoff⁵ has calculated the equilibrium distribution of dislocations and the residual strain in linearly graded composition layers. The calculated density of dislocations in equilibrium is just enough to exactly cancel the lattice mismatch up to a given distance from the interface and the model predicts no dislocations at all above that distance.

In this letter we show that the dislocation distribution of linearly graded composition InGaAs epilayers grown on (001) GaAs substrates by molecular beam epitaxy (MBE) does not coincide with the predicted⁵ equilibrium dislocation distribution. The dislocation density of the dislocation-rich layer thickness is slightly smaller than the equilibrium density. On the other hand, an asymmetric dislocation distribution between the $[110]$ and $[1\bar{1}0]$ directions is observed. An expression is deduced to calculate the residual strain in linearly graded composition layers for the observed (nonequilibrium) situation. This expression is applied to calculate the residual strain at the top surface of a linearly graded composition layer. This calculation makes it possible to suggest a design scheme to grow dislocation-free and unstrained top layers on linearly graded composition buffer layers.

The linearly graded composition InGaAs layers used in

this study were grown by MBE on (001) GaAs substrates at 500 °C. The studied samples consist of a 1 μm thick linearly graded composition InGaAs buffer layer and a 0.3 or 0.5 μm thick uniform composition top layer with varying compositions as shown in Fig. 1.

The dislocation distribution was studied by transmission electron microscopy (TEM) techniques. Specimens were pre-

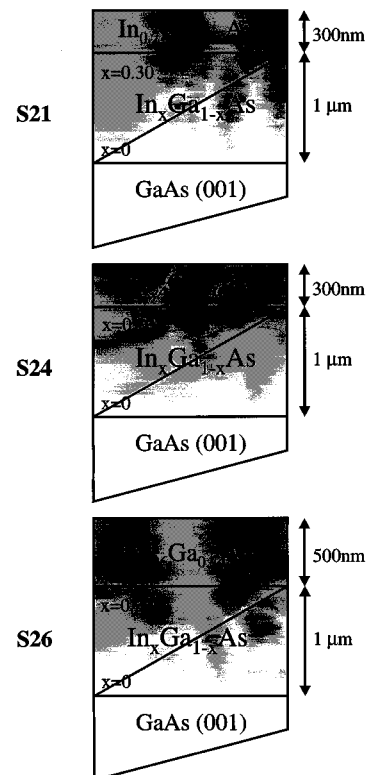


FIG. 1. Scheme of the studied samples.

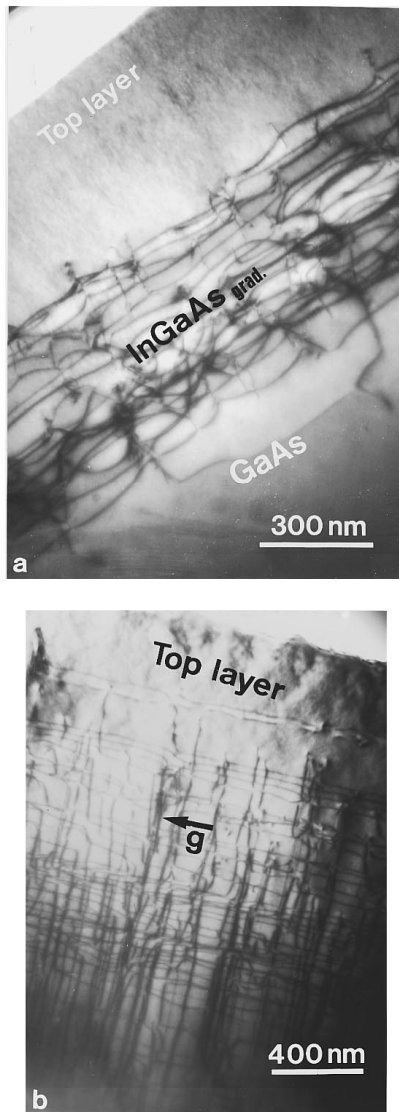


FIG. 2. Bright-field ($g=220$) TEM images of the S21 sample: (a) XTEM; (b) PVTEM.

pared for TEM studies with various techniques: (a) Ar^+ ion milling for cross-sectional TEM (XTEM) observations and (b) chemical etching ($\text{Br}_2 + \text{CH}_3\text{OH}$) for planar-view TEM (PVTEM) studies. TEM observations were performed on Jeol 1200 EX and Jeol 2000 EX transmission electron mi-

croscopes. The dislocation Burgers vectors analysis was fulfilled using the two conventional criteria [$\mathbf{g} \cdot \mathbf{b} = 0$ and $\mathbf{g} \cdot (\mathbf{b} \times \mathbf{u}) = 0$] with the $g_{\{220\}}$, $g_{\{004\}}$, and $g_{\{111\}}$ reflections.

Double crystal x-ray diffraction (DXCRD) rocking curves were obtained for each of the specimens in the surface symmetrical (004) and asymmetrical low and high angle (115) reflections using a Bede Scientific Instrument 150 diffractometer. For each sample four (004) rocking curves were recorded where the projections in the (001) plane of the incident and diffracted beams lie along the four $\langle 110 \rangle$ directions. From these four readings any microscopic tilt between the layer and the substrate was measured, and was corrected for measurements of peak splitting on the corresponding (115) rocking curves. The standard assumptions have been considered to calculate the composition and lattice mismatches.⁶⁻¹⁰ The equilibrium dislocation distribution predicted for a linearly graded composition layer is just enough to exactly cancel the mismatch up to a distance (z_c^{equ}) from the interface and there are no dislocations at all above z_c^{equ} .⁵ The general dislocation distribution observed by TEM in this work is close to the equilibrium distribution, though some significant differences are detected between them:

- (1) The distance z_c from the interface is smaller than z_c^{equ} for both $\langle 110 \rangle$ cross sections.
- (2) The dislocation density (ρ) measured by TEM is slightly smaller than that corresponding to a complete relaxation (ρ_{cr}). This density is identical for the two $\langle 110 \rangle$ cross sections.
- (3) The parameter z_c is different for the two possible $\langle 110 \rangle$ cross sections, i.e., the strain relaxation is not symmetrical.

Figures 2(a) and 2(b) show XTEM and PVTEM images of sample S21, respectively. PVTEM samples were etched only from the bottom side, so that the top layer is visible at the edge of the foil. Similar behavior is observed in samples S24 and S26. This behavior is schematically described in Fig. 3, where the predicted (equilibrium)⁵ and observed dislocation distributions are compared. The parameters z_c are measured for all the studied samples for the two possible $\langle 110 \rangle$ cross sections using XTEM images. Table I shows the graded layer total (z_{tot}), the equilibrium calculated z_c (z_c^{equ})

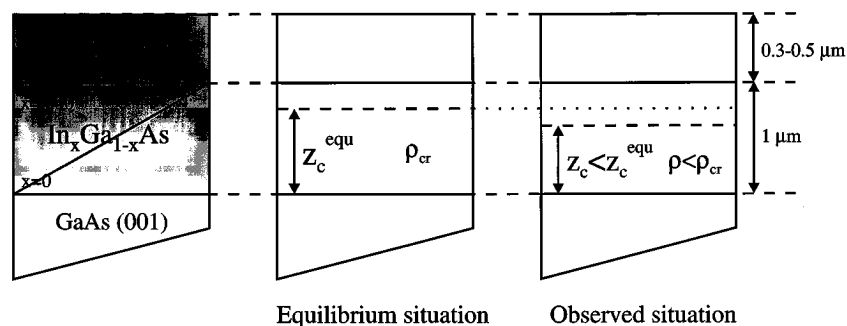


FIG. 3. Schematical representation of the dislocation distribution for the equilibrium and observed situations.

TABLE I. Values of the measured graded layer total (z_{tot}), z_c^A , z_c^B and equilibrium calculated (z_c^{equ}) thicknesses. The three last columns show the relationships $z_c^{\text{equ}}/z_{\text{tot}}$, z_c^A/z_{tot} , and z_c^B/z_{tot} .

Sample	z_{tot} (nm)	z_c^{equ} (nm)	z_c^A (nm)	z_c^B (nm)	$z_c^{\text{equ}}/z_{\text{tot}}$	z_c^A/z_{tot}	z_c^B/z_{tot}
S21	950	817	660	750	0.86	0.69	0.79
S24	950	817	710	810	0.86	0.75	0.85
S26	1060	919	781	890	0.87	0.74	0.84

and the measured z_c (z_c^A and z_c^B) thicknesses. The cross-section A corresponds to the lowest measured z_c parameter, while B corresponds to the remaining one.

Assuming an equilibrium situation, the theoretical residual strain at the top of the graded composition buffer layer (ϵ_r^{equ}) is

$$\epsilon_r^{\text{equ}} = (z_{\text{tot}} - z_c^{\text{equ}}) \epsilon', \quad (1)$$

where z_{tot} represents the total thickness of the linearly graded composition buffer layer and ϵ' is the grading rate ($\epsilon' = d\epsilon/dz$). On the other hand, if the observed dislocation distribution is considered, partial relaxation exists up to z_c , and the residual strain at the top of the graded composition buffer layer (ϵ_r) is

$$\epsilon_r = z_{\text{tot}} \epsilon' - z_c b \rho, \quad (2)$$

where ρ is the mean measured (by TEM) dislocation density below z_c and b is the average misfit composition of the Burgers vector of the dislocations.

Both 60° and 90° perfect dislocations are observed by TEM. The maximum dislocation density is $7 \times 10^9 \text{ cm}^{-2}$ and this density is quite uniform throughout the buffer layer dislocation-rich regions; the observed maximum density difference is lower than $2 \times 10^9 \text{ cm}^{-2}$. Additional TEM measurements have been carried out to calculate the density of each type (60° and 90°) of dislocations; the percentage of 90° dislocations ranges between 22% and 38%. The Eq. (2) allows us to determine the existing lattice (strained) parameter at the top of the graded buffer layer, and then a composition whose lattice parameter will match that at the top of the buffer layer is chosen, so that a layer of this composition will grow with no strain. As the dislocation density at the top of the graded composition buffer layer, measured from PVTEM images, is smaller than 10^5 cm^{-2} , this approach makes it possible to grow an unstrained and dislocation-free ($< 10^5 \text{ cm}^{-2}$) epilayer on top of the graded layer (Fig. 1). Assuming an equilibrium situation [Eq. (1)], the composition of an unstrained top layer has to be $x^{\text{equ}} = 26.0 \pm 0.3\%$. The sample S26 corresponds to this situation. Considering the observed situation ($\rho < \rho_{\text{cr}}$, $z_c < z_c^{\text{equ}}$) the top layer composition required to reach an unstrained state must be smaller than $x^{\text{equ}} = 26.0$. Equation (2) permits to calculate the real residual strain at the top of the graded composition buffer layer, and therefore it is possible to calculate the composition of an unstrained top layer. Using this approach, the calculated x values ($x = x_{\text{tl}}$) considering the measured z_c parameters (see Table I) and dislocation densities of the buffer layer of S26 sample are $x_{\text{tl}}^A = 19.8 \pm 1.2$ and $x_{\text{tl}}^B = 22.5 \pm 1.5$. This x_{tl} value asymmetry, induced by the different values of z_c in the two $\langle 110 \rangle$ directions, implies that the strain in the

TABLE II. Mean strain relaxation and composition data obtained by DCXRD from the top layers.

	Relaxation (%)	Composition (%)
S21	94 ± 5	20.5 ± 1
S24	88 ± 5	22.5 ± 1
S26	80 ± 5	26.5 ± 1

top layer possesses some asymmetry, as expected for the existence of α and β dislocations.¹¹ Since the x_{tl} values are close for both $\langle 110 \rangle$ directions, if the top layer is grown with a composition equal to the mean value (x_{mtl}) of x_{tl}^A and x_{tl}^B , $x_{\text{mtl}} = 21.2 \pm 1.4$, the effects of the asymmetry will be averaged and the layer will grow almost unstrained for both $\langle 110 \rangle$ directions. Sample S21 has been grown to test the validity of this design scheme. To quantify the strain at the top layers of the three grown samples, DCXRD measurements were carried out. The mean strain relaxation data of the top layers, obtained by DCXRD, are shown in Table II. The composition data shown in Table II have been obtained from the strained lattice parameters measured by DCXRD using the standard assumptions.⁶⁻¹⁰ As expected, (1) the top layer is not completely unstrained when an equilibrium situation is assumed, and (2) the relaxation percentage increases as the top layer composition is closer to the predicted average composition value of $x_{\text{mtl}} = 21.2$.

In conclusion, a design scheme of buffer layers is elaborated allowing to grow unstrained and dislocation-free ($< 10^5 \text{ cm}^{-2}$) InGaAs uniform composition epilayers on GaAs substrates using linearly graded composition InGaAs buffer layers. This scheme is developed considering the nonequilibrium situation that these graded composition layers possess.

This work was supported by the CE, under the BLES ESPRIT Project, by the ‘‘Comisi3n Interministerial de Ciencia y Tecnolog3a,’’ CICYT, and by the ‘‘Junta de Andaluc3a,’’ under the group 6020. The work was carried out at the Electron Microscopy Facilities of the University of C3diz.

¹K. Nozawa and Y. Horikoshi, Jpn. J. Appl. Phys. **30**, L668 (1991).

²J. S. Whelan, T. George, E. R. Weber, S. Nozaki, A. T. Wu, and M. Umeno, J. Appl. Phys. **68**, 5115 (1990).

³J. C. P. Chang, T. P. Chin, C. W. Tu, and K. L. Kavanagh, Appl. Phys. Lett. **63**, 500 (1993).

⁴S. I. Molina, G. Guti3rrez, A. Saced3n, E. Calleja, and R. Garc3a, Mater. Res. Soc. Symp. Proc. **325**, 223 (1993).

⁵J. Tersoff, Appl. Phys. Lett. **62**, 693 (1993).

⁶J. Hornstra and W. J. Bartels, J. Cryst. Growth **44**, 513 (1978).

⁷M. A. G. Halliwell, *Advances in X-Ray Analysis*, edited by C. S. Barrett (Plenum, New York, 1990), Vol. 33, p. 61.

⁸L. K. Howard, P. Kidd, and R. H. Dixon, J. Cryst. Growth **125**, 281 (1992).

⁹P. Kidd, P. F. Fewster, N. L. Andrew and D. J. Dunstan, Inst. Phys. Conf. Ser. **134**, 585 (1993).

¹⁰P. Kidd and R. H. Dixon, Inst. Phys. Conf. Ser. **117**, 661 (1991).

¹¹B. A. Fox and W. A. Jesser, J. Appl. Phys. **68**, 2744 (1990).